

CHARACTERIZATION AND MODELING OF RANDOM VECTOR NETWORK ANALYZER MEASUREMENT ERRORS^{*}

Arkadiusz Lewandowski[†], Dylan Williams[‡]

Abstract: We present a technique for characterizing and modeling random vector network analyzer measurement errors. These errors manifest themselves as random changes or drift of vector network analyzer calibration coefficients. We model a change of calibration coefficients as a set of small electrically lumped perturbations occurring at different locations in the vector network analyzer. We then use measurements of a highly reflective offset termination to determine electrical parameters and locations of these perturbations. Our technique is the first step toward developing a statistical description of random vector network analyzer measurement errors and accounting for them in the measurement uncertainty analysis.

I. Introduction

We present a technique for characterizing and modeling random vector network analyzer (VNA) measurement errors. These errors manifest themselves as random changes of the VNA's calibration coefficients and are caused primarily by temperature and humidity drift, cable flexure, imperfect connector repeatability, noise and power-level fluctuations [1]. Our technique provides a useful tool for characterizing these changes. It is also the first step toward developing a statistical description of these changes and accounting for them in the VNA measurement uncertainty analysis.

We model the change of the calibration coefficients as a set of small electrically lumped perturbations occurring at different distances from the reference plane. We describe each of these perturbations with a lumped-element equivalent circuit, as proposed in [2]. However, we extend the approach of [2], which was intended only for describing imperfect connector repeatability, by also identifying the perturbations that occur away from the reference plane. In this way we can account for changes of the electrical parameters of the VNA taking place inside the cables, connectors and the VNA itself.

We characterize the change of the calibration coefficients using a highly reflective offset termination (*e.g.*, offset short or offset open), as proposed in [2]. We compare repeated measurements of the termination, taken as the calibration coefficients change. From the difference of those measurements we determine parameters that model perturbations responsible for the change (*i.e.*, locations of the perturbations and their electrical parameters). We propose a new approach for identifying these parameters that is based on a linear least-squares estimation technique and iterative analysis. Finally, we verify our technique with experimental results.

The main application of our technique is in development of a statistical description for random changes of the VNA's calibration coefficients. Here, we use an example of cable flexure to illustrate. When our technique is used an offset termination is connected to the cable and measured multiple times. Before each measurement, the cable is placed in a new and randomly chosen position and then parameters of the electrical model describing the measured change of the calibration coefficients are identified. A statistical description for the variation of these parameters is then developed, forming a statistical model for the changes of the calibration coefficients due to cable flexure. In a similar way, changes due to drift and imperfect connector repeatability can also be statistically characterized.

The approach for the statistical characterization of random changes of the VNA's calibration coefficients that we suggest differs from the typical approach based on the multivariate analysis of variance [3]. In the typical approach one performs repeated VNA calibrations and then identifies statistically independent mechanisms that contribute to the random changes of the calibration coefficients. Each of these components is then characterized with a covariance matrix describing the uncertainty of the calibration coefficients due to this component.

The advantage of the multivariate analysis of variance is that it delivers a complete and rigorous description of random measurements errors. However, due to the large number of measurements required, it is difficult to implement in practice. This is also a purely statistical approach, and provides no insight into the physics of the errors.

The approach we pursue is easier to implement in practice. It requires only a single reflection-coefficient measurement to characterize the change of the calibration coefficients, making it easier to independently analyze

^{*} This work is a publication of the National Institute of Standards and Technology (NIST), an agency of the U.S. government, and is not subject to U.S. copyright.

[†] A. Lewandowski is with the Warsaw University of Technology, Institute of Electronic Systems, Warsaw, Poland. He is currently a Guest Researcher at NIST, Boulder, CO (e-mail: a.lewandowski@ieee.org).

[‡] D. Williams is with the National Institute of Standards and Technology, Boulder, CO (e-mail: dylan@ieee.org).

changes due to different error mechanisms. However, this approach is approximate, since our model puts restrictions on the electrical character of the change of the calibration coefficients we can capture. At the same time, though, we can gain a better understanding of the physical mechanisms underlying the observed changes.

II. Theory

Our technique for characterizing and modeling changes in the calibration coefficients of the VNA relies on the “error-box” representation of VNA errors [4]. This representation uses electrical two-ports, commonly referred to as error-boxes, to describe the electrical behavior of each of the VNA’s ports (*i.e.*, cables, couplers and receivers). For VNAs with more than one port, this representation is augmented with additional terms accounting for the cross-talk between the ports and errors introduced by the switch that connects the source to the ports. These terms are usually small, and we neglect them in our analysis.

As the error-box description is identical for each port, we can develop our technique by focusing on a single port. We propose a model for error-box changes and then analyze how these changes affect corrected VNA measurements. Then, we develop a procedure for identifying the parameters of the model. The procedure is based on reflection-coefficient measurements of a highly reflective offset termination.

A. Model for error-box changes

We base our model for error-box changes on the assumption that the error-box itself can be modeled as a set of electrically lumped discontinuities connected with transmission-line sections. Therefore, we postulate that a small change of the error-box parameters can be represented by a set of lumped-element perturbations that occur at different fixed locations in the VNA. The circuit in Figure 1 models a single perturbation and consists of small perturbations of the shunt capacitance δC , series inductance δL , series resistance δR , and characteristic impedance δZ_0 . Perturbations δC , δL , and δZ_0 are frequency independent. The resistance perturbation δR is a sum of two components: a frequency-independent change of the DC resistance, δR_{DC} , and a change of the skin-depth resistance $\delta R_{RF} = \delta R_{RF,0}(f/f_0)^{1/2}$, where $\delta R_{RF,0}$ is the skin depth resistance at the reference frequency f_0 . The circuit in Figure 1 can describe several different types of perturbations. For example, the shunt capacitance and the series resistance and inductance can model small length changes of a transmission-line section. These same elements can also model small changes of the electrical parameters of discontinuities. The transformer can model small changes of transmission-line characteristic impedance.

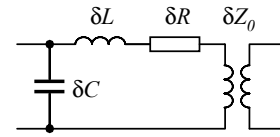


Figure 1. Equivalent circuit for a single perturbation of error-box parameters.

In the following, we analyze how these small perturbations affect corrected VNA measurements. We first consider a single perturbation that occurs at some arbitrary location inside the VNA and is described with the equivalent circuit shown in Figure 1. We analyze the de-embedding procedure and determine a resulting change of a corrected VNA measurement. Finally, we consider all of the perturbations and determine the overall error in corrected VNA measurements.

In the following, we analyze how these small perturbations affect corrected VNA measurements. We first consider a single perturbation that occurs at some arbitrary location inside the VNA and is described with the equivalent circuit shown in Figure 1. We analyze the de-embedding procedure and determine a resulting change of a corrected VNA measurement. Finally, we consider all of the perturbations and determine the overall error in corrected VNA measurements.

Consider a calibrated one-port VNA with an error box described by a transmission matrix \mathbf{T} . After some period the VNA error-box parameters change to a new transmission matrix \mathbf{T}' . We assume that the change is due to a small perturbation that has occurred at some location inside the error-box. We describe the perturbation with a transmission matrix $\Delta\mathbf{T}_n$ (scattering matrix $\Delta\mathbf{S}_n$), where n is the index of the perturbation. For small perturbations of δC , δL , δR , and δZ_0 we can write approximately

$$\Delta\mathbf{T}_n \approx \begin{bmatrix} 1 - \epsilon_{T,n} & \epsilon_{R1,n} \\ -\epsilon_{R2,n} & 1 + \epsilon_{T,n} \end{bmatrix}, \quad \Delta\mathbf{S}_n \approx \begin{bmatrix} \epsilon_{R1,n} & 1 - \epsilon_{T,n} \\ 1 - \epsilon_{T,n} & \epsilon_{R2,n} \end{bmatrix}, \quad (1)$$

where $\epsilon_{R1,n}$, $\epsilon_{R2,n}$ and $\epsilon_{T,n}$ are small numbers. The numbers $\epsilon_{R1,n}$, $\epsilon_{R2,n}$ and $\epsilon_{T,n}$ are, to first order, linear combinations of $\omega\delta C$, $\omega\delta L$, δR and δZ_0 .

In order to express \mathbf{T}' using $\Delta\mathbf{T}_n$, we split the error box \mathbf{T} into two parts. We describe the part between the raw measurement plane and the plane, where the perturbation in Figure 1 is located, with a matrix \mathbf{T}_1 . The remaining part of the error box is represented by a matrix \mathbf{T}_2 . Thus we can write $\mathbf{T} = \mathbf{T}_1\mathbf{T}_2$ and $\mathbf{T}' = \mathbf{T}_1\Delta\mathbf{T}_n\mathbf{T}_2$.

We represent the error in corrected VNA measurements due to the perturbation $\Delta\mathbf{T}_n$ by cascading a transmission matrix $\Delta\mathbf{T}_{e,n}$ with the error-box transmission matrix \mathbf{T} . Thus, we can write the matrix $\Delta\mathbf{T}_{e,n}$ as

$$\Delta\mathbf{T}_{e,n} = \mathbf{T}^{-1}\mathbf{T}' = (\mathbf{T}_1\mathbf{T}_2)^{-1} \mathbf{T}_1\Delta\mathbf{T}_n\mathbf{T}_2 = \mathbf{T}_2^{-1}\Delta\mathbf{T}_n\mathbf{T}_2. \quad (2)$$

In order to expand (2) we make use of the assumption, made earlier, that the error-box can be seen as a set of electrically lumped discontinuities connected with transmission-line sections. Hence, we can write approximately

$$\mathbf{T}_2 = \prod_{i=1}^n \mathbf{T}_{2,i}, \quad \mathbf{T}_{2,i} \approx \begin{bmatrix} (1 - \delta_{T,i})e^{-j\beta l_{n,i}} & \delta_{R1,i} \\ -\delta_{R2,i} & (1 + \delta_{T,i})e^{j\beta l_{n,i}} \end{bmatrix}, \quad (3)$$

where $\delta_{R1,i}$, $\delta_{R2,i}$ and $\delta_{T,i}$ are small numbers, β is the propagation constant, $l_{n,i}$ is the physical length of the i -th section, i is the index of the section. By inserting (3) into (2) and considering only first-order terms we obtain

$$\Delta \mathbf{T}_{e,n} \approx \begin{bmatrix} 1 - \varepsilon_{T,n} & \varepsilon_{R1,n} e^{j2\beta l_n} \\ -\varepsilon_{R2,n} e^{-j2\beta l_n} & 1 + \varepsilon_{T,n} \end{bmatrix}, \quad (4)$$

where $l_n = l_{n,1} + \dots + l_{n,M}$ is the distance of the perturbation from the reference plane. Finally, since we assumed that the perturbations are small, we can neglect multiple reflections and write the overall error as the linear combination

$$\Delta \mathbf{T}_e \approx \begin{bmatrix} 1 - \sum_{n=0}^N \varepsilon_{T,n} & \sum_{n=0}^N \varepsilon_{R1,n} e^{j2\beta l_n} \\ -\sum_{n=0}^N \varepsilon_{R2,n} e^{-j2\beta l_n} & 1 + \sum_{n=0}^N \varepsilon_{T,n} \end{bmatrix}, \quad (5)$$

where $N+1$ is the number of perturbations. We assume that $l_0=0$, which corresponds to a perturbation at the reference plane.

Expression (5) describes the overall error in corrected VNA measurements due to small perturbations occurring inside the VNA error box. It shows that, to first order, this error depends only on the electrical parameters of the perturbations and their distances from the reference plane, and is independent of the calibration coefficients. Moreover, the transmission terms of the matrix $\Delta \mathbf{T}_e$ do not depend on the distance of the perturbation from the reference plane, whereas the reflection terms are multiplied only by an additional phase-shift term corresponding to the round trip of the signal between the reference and perturbation planes.

B. Determination of model parameters

We determine parameters of the model for VNA error-box changes using reflection-coefficient measurements of a highly reflective offset termination. We perform two different corrected measurements Γ_1 and Γ_2 of the termination. The difference between the measurements results from the change of VNA error-box parameters. Therefore, we use Γ_1 and the coefficient of the matrix $\Delta \mathbf{T}_e$ to approximate Γ_2 . From that, we determine the locations and electrical parameters of the perturbations that underlie the change of VNA error-box parameters.

The relationship between Γ_2 , Γ_1 and $\Delta \mathbf{T}_e$ corresponds to the transformation of Γ_1 through the transmission matrix $\Delta \mathbf{T}_e$. Therefore, we can write the approximation $\Gamma_{2,m}$ of the reflection coefficient Γ_2 as

$$\Gamma_2 \approx \Gamma_{2,m} = \frac{\Delta T_{e,12} + \Delta T_{e,11} \Gamma_1}{\Delta T_{e,22} + \Delta T_{e,21} \Gamma_1}. \quad (6)$$

Relationship (6) is a non linear function of the perturbation locations (*i.e.*, l_n , for $n=1, \dots, N$) and their electrical parameters (*i.e.*, δC , δL , δR , and δZ_0). However, if we consider only first-order terms, we can write (6) approximately as a linear function of perturbation electrical parameters δC , δL , δR , and δZ_0 .

For given Γ_1 , Γ_2 and set of frequencies, we find the locations of the perturbations and their electrical parameters by minimizing the mean-square error between the approximation $\Gamma_{2,m}$ and the measurement Γ_2 . We need to proceed iteratively because of the nonlinear dependency of $\Gamma_{2,m}$ on the locations l_n , for $n=1, \dots, N$ of the perturbations. We begin with estimates of these locations. We obtain these estimates either from the knowledge of the VNA's design, or analysis of $\Delta \Gamma = \Gamma_2 - \Gamma_1$ in the time domain. At each iteration, we first calculate the electrical parameters of the perturbations by means of a linear least-squares technique. Then, we refine the location estimates. To this end we fix the perturbation parameters, linearize the dependency of $\Gamma_{2,m}$ on l_n for $n=1, \dots, N$, and determine the location corrections with a linear least-squares technique. We continue the procedure until the mean-square error becomes smaller than a prescribed convergence threshold.

III. Experiments

We verified our method for characterizing VNA random errors with measurements of VNA drift. We calibrated a two-port VNA equipped with a 1.85 mm coaxial connector up to 67 GHz. One of the VNA ports had no cable attached to it and we used this port for our measurements. We performed corrected measurements of a 5.1 mm long offset short over a period of time. We measured the short immediately after the calibration and then after 1 hour and 3.5 hours. The short was not disconnected between measurements.

The measured relative change of reflection coefficient is shown in Figure 2 along with results from the model. The real and imaginary parts of $\Delta \Gamma / \Gamma_1$ correspond to changes in magnitude and phase, respectively. The slope and variation of the measured imaginary part of $\Delta \Gamma / \Gamma_1$ are modeled very accurately. The real part of $\Delta \Gamma / \Gamma_1$ is modeled less accurately. However, in both cases the real part of $\Delta \Gamma / \Gamma_1$ is much smaller than the imaginary part of $\Delta \Gamma / \Gamma_1$. This indicates that the drift is caused primarily by reactive effects, such as changes in cable length. We also see in Figure 2 that the imaginary part of $\Delta \Gamma / \Gamma_1$ and the ripples in both the real and imaginary part are larger after 3.5 hours than after 1 hour. This indicates that the drift increases with time.

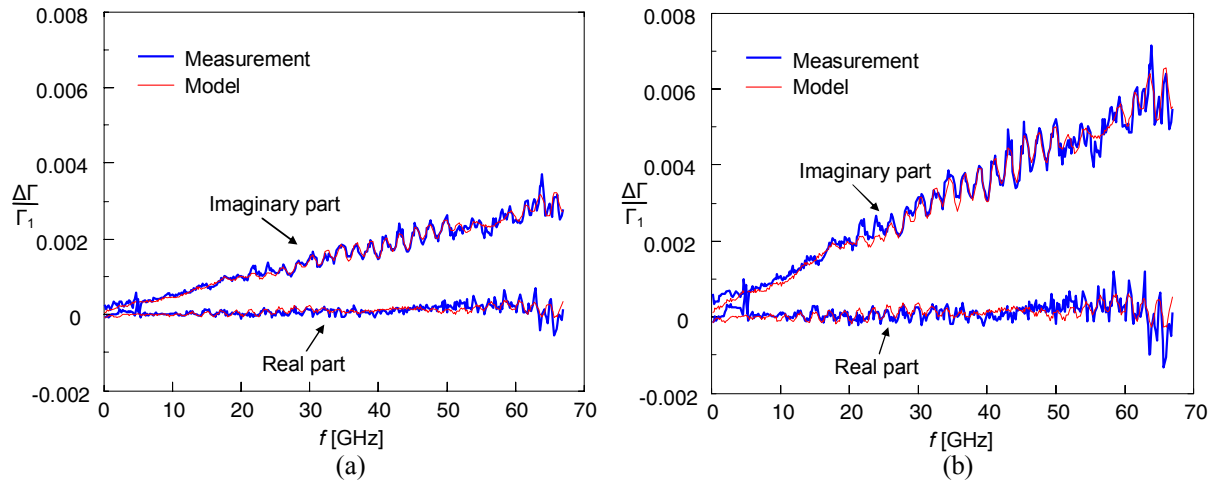


Figure 2. Drift of corrected VNA measurements of a 5.1 mm offset short (a) after 1 hr and (b) after 3.5 hrs; measurement (thick blue line) and model (thin red line).

We modeled the measurement results with seven perturbations. We used the same locations of the perturbations for both measurements. We estimated these locations from a time-domain representation of the difference between the measured reflection coefficients, and then refined them in the modeling procedure. Both sets of values are presented in Table 1. Our initial estimates from the time-domain analysis are close to optimized values.

For each perturbation we determined parameters of the equivalent circuit in Figure 1. One of these parameters is the difference between the normalized inductance

$\delta l = \delta L/Z_{ref}$ and the normalized capacitance $\delta c = \delta C Z_{ref}$, where Z_{ref} is the reference impedance. We show this parameter in Table 2. This parameter attains its largest value at the distance $d = 66.18$ mm from the reference plane. This distance corresponds to a ripple period of $\Delta f = c/(2d) \approx 2.2$ GHz, where c is the speed of light in air. This agrees very well with the period observed in the measurements in Figure 2. We also see that for all perturbations, except the furthest one, the absolute value of the difference $\delta l - \delta c$ is larger after 3.5 hours than after 1 hour. This confirms the observation that the drift increases with time.

Table 1. Locations of the perturbation: initial estimates and final values after modeling.

	l_1 [mm]	l_2 [mm]	l_3 [mm]	l_4 [mm]	l_5 [mm]	l_6 [mm]
Estimated	5.00	30.00	62.00	65.00	67.00	329.00
Modeled	5.21	30.68	62.37	65.54	66.18	328.60

Table 2. Selected perturbation parameters.

Location [mm]	$\delta l/Z_{ref} - \delta c Z_{ref} [10^{-15}/\text{Hz}]$						
	0	5.21	30.68	62.37	65.54	66.18	328.60
After 1 hr	0.036	0.481	-0.263	0.697	-0.900	2.344	0.097
After 3.5 hrs	0.196	0.696	-0.583	1.431	-2.010	4.863	0.072

IV. Conclusions

In this work, we presented an approach for characterizing and modeling random VNA measurement errors. Our approach is based on a model consisting of multiple lumped-element perturbations located at different fixed distances from the reference plane. Parameters of the model are identified by means of standard linear techniques, based on only a single measurement of a highly reflective offset termination. The use of a single measurement to characterize the change of VNA electrical parameters simplifies the characterization of the statistical properties of random VNA measurement errors due to drift, cable flexure, or imperfect connector repeatability. We demonstrated our approach by characterizing and modeling the drift of VNA electrical parameters over a period of time. Our model was able to accurately reproduce the measurements.

References

- [1] Rytting, D. K., "Network Analyzer Accuracy Overview," *ARFTG Conference Digest-Fall, 58th*, vol.40, pp.1-13, Nov. 2001.
- [2] Juroshek, J.R., "A Study of Measurements of Connector Repeatability Using Highly Reflecting Loads," *Microwave Theory and Techniques, IEEE Transactions on*, vol.35, no.4, pp. 457-460, Apr. 1987.
- [3] Mendenhall, W., Sincich, T., *Statistics for engineering and the Sciences*, 5th ed., Prentice Hall, 2006.
- [4] Rytting, D. K., "An Analysis of Vector Measurement Accuracy Enhancement Techniques," *RF & Microwave Symposium and Exhibition*, 1980.